GEOMETRIC MODEL OF LARGE SCALE STRUCTURES IN THE MAGNETOSPHERE

http://helio.estec.esa.nl/Cluster-2/index.html

Hugh D. R. Evans[1, 2], Lisa Rosenqvist[3], Alain Hilgers[2]

[1] Rhea System SA, Avenue Einstein 2a, B-1348 Louvain-la-Neuve, Belgium,
phone: +31 71 565-5109, fax: +31 71 565-5420, h.evans@rheagroup.com
[2] Space Environment and Effects Analysis Section, ESTEC, Noordwijk, The Netherlands
[3] Uppsala University, Uppsala, Sweden

Abstract

Large-scale structures of the Earth's magnetosphere are implemented in a tool that provides a simple and efficient geometric model of the magnetosphere. The model is based on previously published statistical models of the bow shock, magnetopause, neutral sheet and plasma sheet. The seasonal and diurnal effects of the variation of the Earth's magnetic dipole and the solar wind speed and density are included in the modelling of the structures. The solar wind data from the ACE spacecraft can be included in the model to provide a near real-time view of the magnetosphere. The model has been used to identify crossings of these large structures for the Cluster-2 mission and to identify the duration of plasma sheet crossings for the XMM/Newton spacecraft.

Introduction

The Earth plasma environment is strongly organised in large-scale structures with specific plasma properties. To determine the type and the magnitude of spacecraft-plasma interactions, spacecraft designers and spacecraft operators require models of these large-scale structures.

A visualisation tool for the large-scale structures of the magnetosphere has been implemented in the Virtual Reality Modelling Language (VRML) [1] and the Java programming language. This provides a WWW based interface to the magnetospheric models that can be accessed with a standard web browser (Internet Explorer) and the Cortona VRML plug-in [2].

Bow Shock and Magnetopause

The Bow Shock is modelled using the Peredo et al. [3] terrestrial bow shock model, and the Magnetopause is modelled using the Fairfield Meridian 4° model [4]. This model assumes the bow shock to be a cylindrically symmetric conic section translated and rotated into the Earth centred Geographic Solar Ecliptic (GSE) co-ordinate system, see Figure 1. The conic section is represented in the form

$$\frac{L}{r} = 1 + \varepsilon \cos\theta$$

in which L is the semilatus rectum, and ε is the eccentricity of the conic. The variables r and θ are polar co-ordinates in the natural system for the conic ([x^{abd}, y^{abd}] in Figure 1, below). This native system is abberated by an angle α from GSE, such that tan (α)= $V_{Earth's\ orbital\ motion}$ / $V_{solar\ wind}$. The co-ordinate system is further displaced from the Earth's centre by $\boldsymbol{r_0}$=[x_0, y_0, 0].

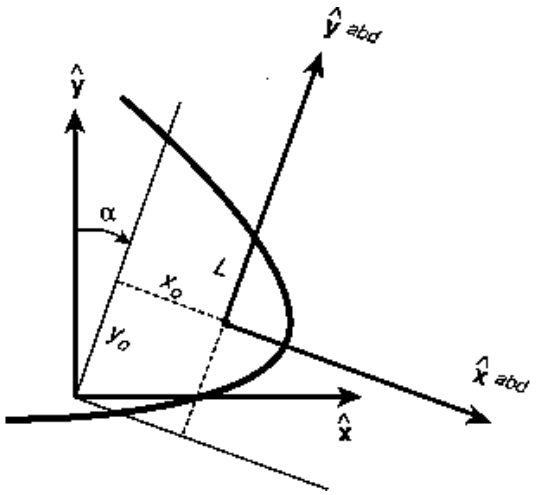

Figure 1. Observational (e.g. GSE) coordinate system (x ,y) and aberrated-displaced system (x^{abd}, y^{abd}) for model boundaries. The direction of α is defined such that positive values correspond to the aberration from the Earth's orbital motion, which is in the ***-y*** *direction.*

To account for the variation of the model with the solar wind dynamic pressure L and $\boldsymbol{r_0}$ are scaled by a factor s_{sw} by the solar wind dynamic pressure, ρ_{sw}:

$$s_{sw} = \left(\frac{\rho_{sw}}{\rho_0} \right)^{-\frac{1}{6}}$$

This factor serves to model the balance of the magnetic pressure exerted by the Earth's dipole field with the dynamic solar wind pressure. The average solar wind dynamic pressure, the normalisation constant ρ_0, is specified as 3.1 nPa by the Peredo bow shock model. The Fairfield magnetopause model, however, does not specify this constant, and so 3.1 nPa is assumed, for consistency with the Peredo model.

The 3D conic sections are modelled in the VRML language as a circle in the (y^{abd}, z^{abd}) plane extruded along the $-x^{abd}$ axis. The radius of the circle is scaled by the y^{abd} component of the magnetospheric model to form the shape of the conic section. The conic section is then translated and rotated about the y-axis into the GSE co-ordinate system. The entire construct is then spatially scaled for the variation of the solar wind dynamic ram pressure.

Table 1. Conic section and aberration parameters for the bow shock and magnetopause models.

	Bow Shock	Magneto-pause
	Peredo et al.	Fairfield Meridian 4°
L (R_{Earth})	26.1	13.1
ε	0.98	0.79
$\boldsymbol{R_0}$=[x_0, y_0] R_{Earth}	[2, 0.3]	[3.6, 0.4]
ρ_0 (nPa)	3.1	(3.1)
$V_{Earth's\ orbital\ Motion}$ (km/s)	30	30

Neutral Sheet - Tail ward Extrusion

The neutral sheet is the locus of points where the magnetic field intensity reaches a minimum and the component of the magnetic field measured along the Earth-Sun axis reverses in sign [5]. The exact position of the neutral sheet is essentially determined locally, when a spacecraft traverses it. However, a large set of neutral sheet crossings can be used to generate a time dependent model of the neutral sheet.

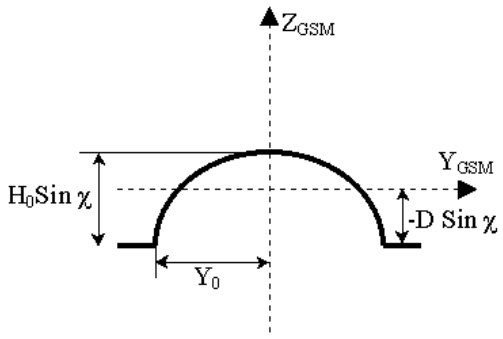

Figure 2. Cross-section of the magnetotail showing the displaced ellipse neutral sheet model.

Fairfield presents a model where the neutral sheet is represented as a tail ward projection of an ellipse, which is tilted at an angle χ to the solar magnetospheric plane and with a displaced centre north or south of the Sun-Earth X-axis depending on the tilt angle, see Figure 2.

The model describes the displacement of the centre of the ellipse, δZ, by the following:

For $Y_{GSM} < Y_M$:

$$\delta Z = \left[(H_0 + D)\left(1 - \left(\frac{Y_{GSM}}{Y_M}\right)^2\right)^{\frac{1}{2}} - D \right] \sin\chi$$

For $Y_{GSM} >= Y_M$:

$$\delta Z = -D \sin\chi$$

The structure is modelled in geocentric solar magnetospheric co-ordinates (GSM). The constant Y_M describes the width of the arched surface and the parameter D represents the displacement of the centre of the curve above or below the abberated X_{GSM} axis. The constant H_0, called the "hinging distance", is the distance from the Earth at which the X-independent surface in the tail is attached to the geomagnetic equator.

Fairfield [6] has derived the values of the constants D, H_0, and Y_M that provide a best fit of the measurements from IMP-6 and IMP-7 and are, thus, best adapted to geocentric distances between 30 and 40 R_{Earth}. However, for the near-Earth region (< 22.6 R_{Earth}), the Gosling et al. parameters [7], which provide a fit to the ISEE-2 data from 1978, are better suited to the neutral sheet model for orbits such as Cluster-2, see Table 2.

Table 2. Parameters for the elliptic tail ward extrusion for the neutral sheet model. All values are in units of Earth radii.

	D	H_0	Y_M
Fairfield	14	10.5	22.5
Gosling	7	9	13.5

The neutral sheet is modelled in VRML in a manner similar to the displaced ellipse neutral sheet model, i.e. as an extrusion of the Fairfield function, above, along the tailward direction, starting at 10 R_{Earth} and continuing to 20 R_{Earth}. The Modified Julian Day 1950 is passed to this construct, from which the χ parameter is calculated.

Dipolar Region of keV electrons

The dipolar part of the magnetosphere, where plasma sheet and inverted "V" electron precipitations are observed, is described in the model by a dipolar magnetic field up to a geocentric equatorial radius of 15 R_{Earth}. This is a simplification, as the Earth's magnetic field may depart substantially from such a dipolar field

at geocentric distances beyond 5 R_{Earth} due to the interaction of the solar wind, which also introduces a strong day/night asymmetry.

In this region below 15 R_{Earth}, magnetic shells are described with the help of the parameter *r*, which is the geocentric distance of the intersection of the magnetic force line with the magnetic equatorial plane. Measurements from polar orbiting spacecraft have shown that plasma sheet and inverted "V" electrons are often encountered in a region extending from r=5 R_E to r=15 R_E [8]. The model of this keV electron region is implemented as a bounding limit magnetic shell with r=15 R_E.

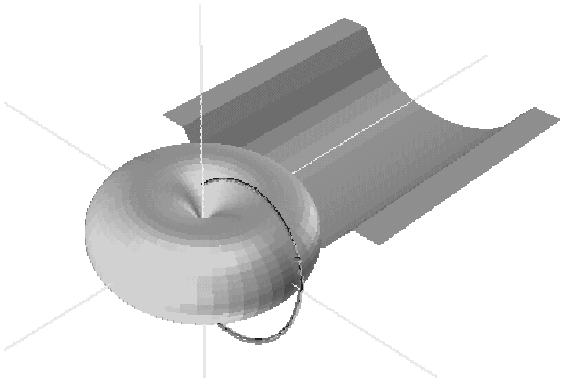

Figure 3. VRML implementation of the Gosling elliptical tailward extrusion and the dipole plasmasheet electron limit in GSE coordinates at 14-Dec-2001 02:00 UT. The Cluster-2 orbits are also shown.

The surface representing the maximum limit of the dipolar region is implemented in VRML as a rotational dipolar extrusion in GSM coordinates. This construct, along with the tailward neutral sheet extrusion, is transformed from GSM coordinates to GSE coordinates, see Figure 3.

Magnetic Field Lines

The IGRF-95 and Tsyganenko 1996 internal and external magnetic field lines are traced in the MAG[1] coordinate system from points located at longitudes of 20° intervals, co-latitude of 25° and geocentric radius of 10000 km. The field lines are traced by a FORTRAN program, which interfaces the WWW to the UNILIB library [9], and converted to VRML. A separate interface allowing full parametric control is available at http://helio.estec.esa.nl/hevans/b_line/.

[1] **Z** is the dipole axis, **Y** is the intersection of the geographic equator and the geographic meridian 90° East of the meridian containing the dipole axis.

The Tsyganenko 1996 external field model requires, as inputs, the $\mathbf{B_Y}$ and $\mathbf{B_Z}$ interplanetary magnetic field (IMF) components (nT), the solar wind pressure (nPa) and the Dst index (nT). For the simulation, only the solar wind pressure and the Dst index are supplied to the calculation. The IMF components are set to 0.

As the conversion of the field line tracing to VRML is a computationally intensive operation, i.e. takes >5 seconds to complete with a fast network connection, the feature is normally disabled to ensure a reasonably quick response from the model when modifying the epoch, solar wind parameters or D_{ST} index from the applet.

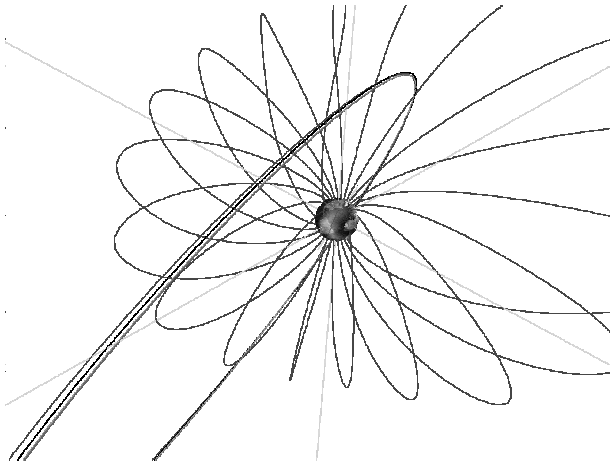

Figure 4. The magnetic field lines calculated from the IGRF-95 internal and the Tsyganenko-96 external magnetic field models. The Cluster-2 trajectory is also shown.

ACE Solar Wind Parameters

To provide a simulation of the state of the magnetosphere, the ACE SWEPAM solar wind data can be automatically included in the simulation. The server downloads the hourly averaged data, provided by NOAA/SEC[2], on an hourly basis and archives it. The data for the month of the simulation's epoch is then served to the simulation. This circumvents the security restriction, imposed by the Java applet run time environment, that prohibits the applet from accessing servers other than that from which it was originally served. The hourly data is provided to reduce the download time, while still providing a near real-time simulation of the magnetosphere.

[2] See ftp://ftp.sec.noaa.gov/pub/lists/ace2/

The solar wind ram pressure, used by several of the models in the simulation, is calculated from the ACE SWEPAM speed and density data using the formula:

$$p_{sw} = C\rho_{sw}V_{sw}^2$$

where, V_{sw} is the solar wind speed, ρ_{sw} is the solar wind density, and C is a constant for conversion to nPa units (1.6726E-6 nPa cm^{-3} km^{-2} s^2). Two definitions of the solar wind dynamic pressure are in use in space physics: the momentum flux (p_{mf}) and the kinetic energy per unit volume (p_{ke}). The momentum flux has its origins in the flow equations that describe conservation of momentum, while the kinetic energy density is usually found in aerodynamics and fluid dynamics and is derived from the conservation of energy in a steady flow. The relation between the two is $p_{ke} = ½\ p_{mf}$. In this simulation, the momentum flux definition is applied.

It is also possible to disable the automatic loading of the ACE SWEPAM data, allowing the user to perform a "what if" analysis by specifying their own values for the solar wind speed and density.

As no easily accessible near real-time Dst index is available on the Internet, the user is required to enter this parameter in the control applet. This parameter, though, only affects the magnetic field line model, and so doesn't greatly diminish the functionality of the simulation. There are several sites (DMI, CRL, and UCLA) that do provide Dst index predictions via the Internet, but the forms in which they are presented do not lend themselves to easy extraction of the indices.

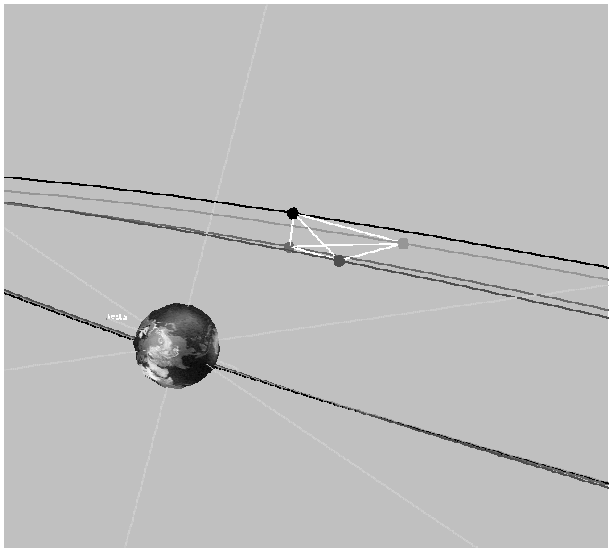

Figure 5. The four Cluster spacecraft, their orbits and the tetrahedron with a spacecraft at each vertex.

Satellite Trajectory

The trajectories of the four Cluster-2 satellites are represented for the epoch of the simulation as elliptical lines that are coded in the standard Science Working Team colours, seen in the following table.

Satellite	Colour
Rumba	Black
Salsa	Red
Samba	Green
Tango	Magenta

The closest ephemera from the Long Term Orbit File (LTOF) is served by a Common Gateway Interface (CGI) script on the server to a Java object which converts it to a GSE state vector. White lines are drawn to represent the tetrahedron formed by the spacecraft positions, see Figure 5.

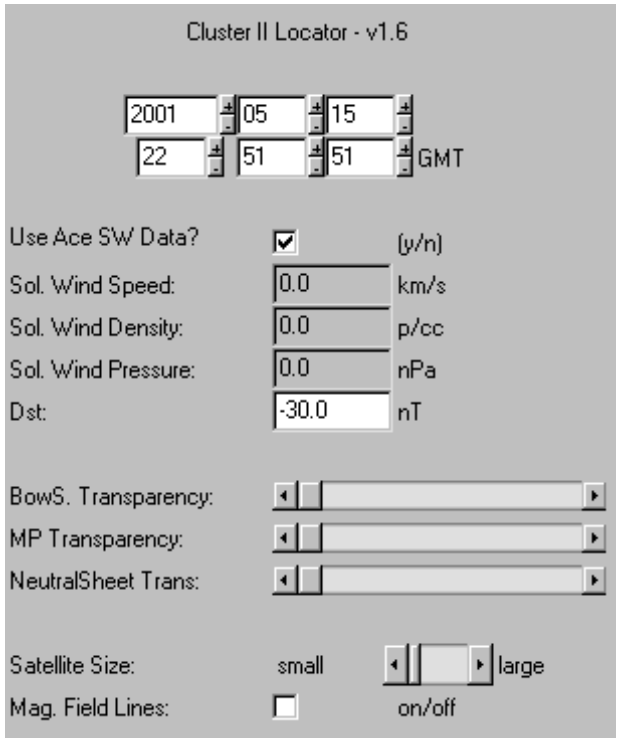

Figure 6. The Java Applet that controls the VRML simulation allows the user to modify the simulation conditions.

The Control Applet

The control applet, see Figure 6, provides the interface to the VRML simulation, allowing the user to modify the simulation's epoch, the solar wind speed and density, the D_{ST} index. In addition, the applet permits the user to modify the transparency of the bow shock,

magnetopause and neutral sheet. Without this ability, it is difficult to easily view the various structures and their positional relationship with the other constructs. The satellite size is similarly variable, to permit quick location from views at great distances while still permitting the finer structure of the tetrahedron and inter-satellite positions to be resolved at closer viewpoints. In addition, the magnetic field line generation can be switched on and off by a simple toggle button.

Several viewpoints are provided by the simulation, the default view from an angle, along the X, Y and Z axes, from the Earth, and from either of the four Cluster satellites. When a Cluster satellite is chosen as the viewpoint, the viewpoint will move with the satellite as the satellite moves with the epoch. This is particularly useful when following the evolution of the tetrahedron or determining the point at which the satellites straddle one of the structures.

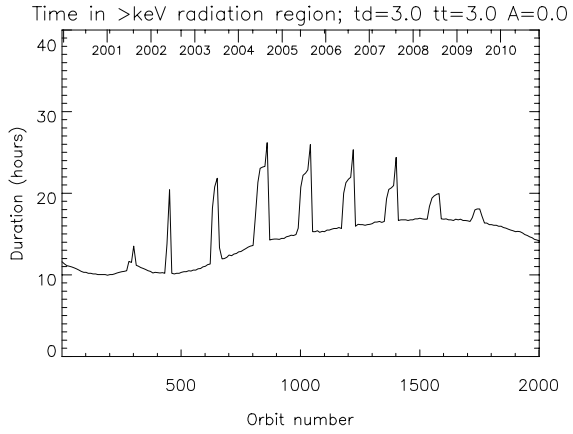

Figure 7. Time spent inside the plasma sheet electron region as a function of the orbit number for a half thickness of the tail plasmasheet and dipolar region equal to 3 R_{Earth}. The smooth part of the curve corresponds to encounters with the dipolar region, while the spikes correspond to the tail plasmasheet encounters.

XMM Plasma Sheet Crossings

The simple geometric models described above can be applied to support mission preparation and mission planning activities. As an example, the neutral sheet model is used to evaluate the possible occurrence of keV electron region crossing by the XMM/Newton spacecraft. Electrons in this energy range may potentially affect the X-ray detector background via X-ray emission in telescope walls. For a given position of the spacecraft, the minimum distance to the centre of the modelled plasma sheet electron region can be calculated as follows. First, the dipole shell parameter, *r*, for XMM corresponding to the spacecraft position is derived from the dipole field equation,

$$r = \frac{R_{XMM}}{\cos^2 \Phi}$$

where Φ denotes the dipolar latitude and R_{XMM} is the distance from the spacecraft to the centre of the Earth. The value $|r_0\text{-}r|$ represents a measure of the distance of the spacecraft from the midshell of plasma sheet electrons dipolar region. If the spacecraft is located at $X_{GSM} < -10\ R_{Earth}$, the value of $|r_0\text{-}r|$ is compared to the elevation of the spacecraft along the Z-axis with respect to the neutral sheet. The minimum of the two values is defined as the distance between the spacecraft and the centre of the region of interest.

This procedure has been applied to 2008 consecutive XMM/Newton orbits from December 1999 to December 2010. Attributing a plasma sheet thickness, e.g. 3 R_{Earth}, permits the duration of the plasmasheet crossings to be calculated, or more specifically, where the risk of encountering plasmasheet electrons is high. In Figure 7, the duration of high risk periods of the orbit are plotted as a function of orbit number. It can be seen that the duration of periods where both dipolar keV region and plasma sheet electron encounters occur, are strongly modulated (50% for the dipolar region and a factor of 2 for the tail plasma sheet encounter). By suppressing the dipole tilt, it can be shown that the dipole inclination is the principle cause of the modulation of the plasma sheet encounters.

Extending the thickness of the keV electron region to 5 R_{Earth} does not qualitatively change these results and the overall aspect of the curve. Further, it is expected that taking into account the compression of the magnetosphere on the noon side would induce a stronger modulation of the low altitude encounter with keV electron regions.

Conclusions

Four models of large structures of the Earth's magnetosphere have been implemented in a VRML/Java system that is available via the Internet. The system can provide a near real-time simulation of the state of the bow shock, magnetopause, and neutral sheet along with the location of the Cluster-2 spacecraft in relation to them. The application of the plasma sheet model to the XMM/Newton orbit has been demonstrated, outlining the value of the model to mission and operations planning.

Further improvements to the modelling will include the upgrading of the plasmasheet dipole model with a more representative *L-shell* model based on the IGRF-95 and Tsyganenko-96 external magnetic field models. The tailward neutral sheet extrusion will be provided with a thickness, instead of the simplified two dimensional elliptic extrusion. More detailed control of the magnetic field model through the IMF B_y and B_z components can be included, as well as the tracing of the magnetic field

line from the spacecraft locations. The inclusion of other spacecraft of interest via the NORAD Two-Line Element (TLE) set would upgrade this tool into a more useful general-purpose simulation.

Acknowledgements

The authors would like to thank NOAA's Space Environment Center for the online provision of ACE solar wind data in a near real time format.

References

[1] "The Virtual Reality Modelling Language", International Standard ISO/IEC 14772-1:1997, http://www.web3d.org/technicalinfo/specifications/vrml97/index.htm

[2] "Cortona VRML Client", Parallelgraphics, http://www.parallelgraphics.com/products/cortona/

[3] Peredo, M et al., "Three-dimensional position and shape of the bow shock and their variation with Alfvenic, sonic and magneto-sonic Mach numbers and interplanetary magnetic field orientation", *J. Geophys. Res.*, **100**, 7907-7916, 1995.

[4] Fairfield, D. H., Average and unusual locations of the Earth's magnetopause and bow shock, *J. Geophys. Res.*, **76**, 6700-6716, 1971.

[5] Ness, N.F., The Earth's magnetic tail, *J. Geophys. Res*, **70**, 2989, 1965.

[6] Fairfield, D. H., A Statistical determination of the shape and position of the geomagnetic neutral sheet, *J. Geophys. Res*, **85**, 775-780, 1980.

[7] Gosling, J. T., McComas, D. J., Thomsen, M.F., Bame, S.J., The warped neutral sheet and plasma sheet in the near-Earth geomagnetic tail, *J. Geophys. Res*, **91**, 7093-7099, 1986.

[8] Sandahl, I., et al., Distribution of Auroral Precipitation at midnight during a magnetic storm, *J. Geophys. Res.*, **95**, 6051-6072, 1990.

[9] Kruglanski, M., UNILIB….

[10] Tsyganenko, N.A. and Stern, D.P., Modeling the global magnetic field the large-scale Birkeland current systems, *J.Geophys.Res*. **101,** 27187-27198, 1996.

[11] Hilgers, A., Gondoin, P., Nieminen, P., Evans, H., Prediction of Plasma Sheet Electron Effects on X-ray Mirror Missions, Proceedings of ESA workshop on Space Weather, WPP-155, ISSN 1022-669, 293-296, ESTEC, The Netherlands, 1999.

[12] Rosenqvist, L., Hilgers, A., Daly, E., Evans, H., Geometric Model of Diurnal and Annual Variation of keV Electron Region Crossings on Highly Eccentric Earth Orbits, submitted to *J. Atmos. And Terr. Phys.,* 2001.

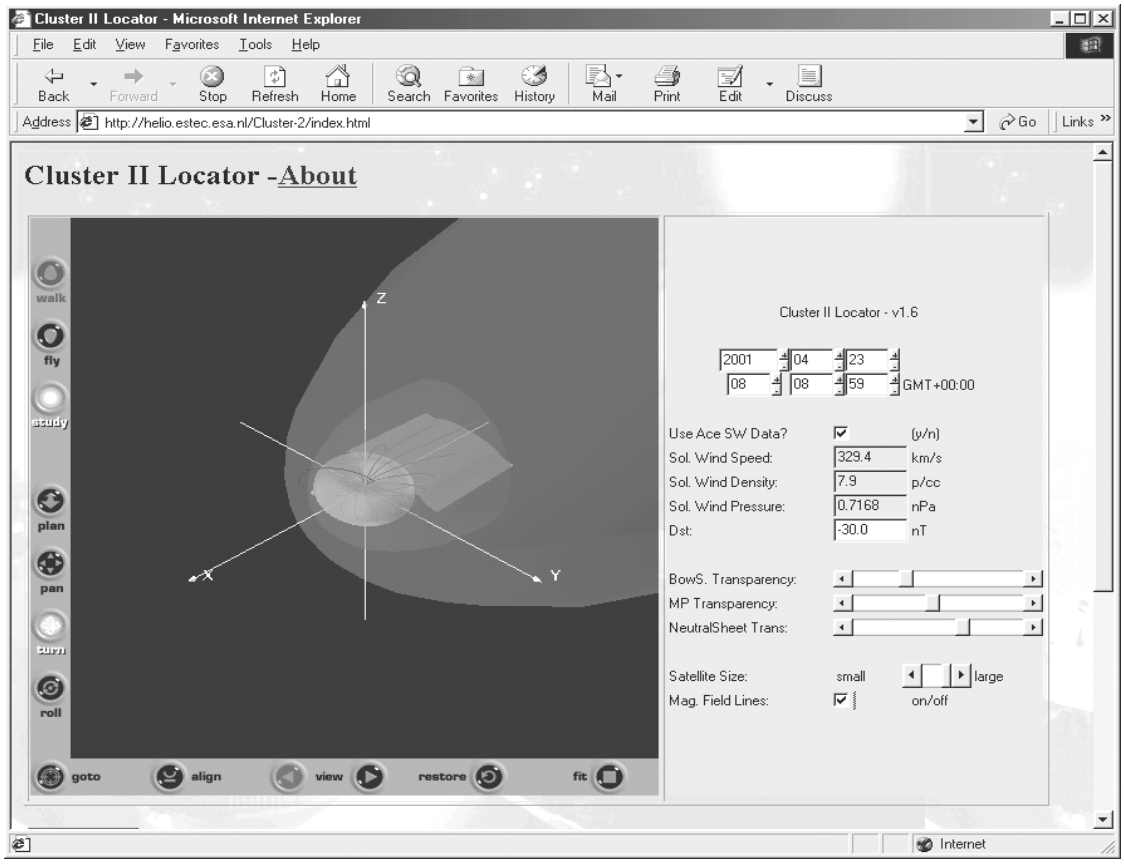

Figure 8. The Cortona VRML plugin (left) with the Java control applet (right).